Stronger evidence for genetic ancestry than environmental conditions in shaping the evolution of a complex signaling trait during biological invasion

Running title

Dewlap evolution in non-native brown anoles

Authors

Jessica N. Pita-Aquino[a], Dan G. Bock[b], Simon Baeckens[c], Jonathan B. Losos[b], and Jason J. Kolbe[a]

Affiliation

[a]Department of Biological Sciences, University of Rhode Island, Kingston, RI 02881

[b]Department of Biology, Washington University in St. Louis, St. Louis, MO 63130

[c]Department of Organismic and Evolutionary Biology, Harvard University, Cambridge, MA 02138

Corresponding author

Jason J. Kolbe, jjkolbe@uri.edu

Present addresses:

Jessica N. Pita-Aquino: Department of Biochemistry, University of Utah School of Medicine, Salt Lake City, UT 84132

Dan G. Bock: Department of Botany and Biodiversity Research Centre, University of British Columbia, Vancouver, BC, V67 1Z4, Canada

Simon Baeckens: Department of Biology, Ghent University, 9000 Gent, Belgium

Abstract

Introductions of invasive species to new environments often result in rapid rates of trait evolution. While in some cases these evolutionary transitions are adaptive and driven by natural selection, they can also result from patterns of genetic and phenotypic variation associated with the invasion history. Here, we examined the brown anole (*Anolis sagrei*), a widespread invasive lizard for which genetic data have helped trace the sources of non-native populations. We focused on the dewlap, a complex signaling trait known to be subject to multiple selective pressures. We measured dewlap reflectance, pattern, and size in 30 non-native populations across the southeastern United States. As well, we quantified environmental variables known to influence dewlap signal effectiveness, such as canopy openness. Further, we used genome-wide data to estimate genetic ancestry, perform association mapping, and test for signatures of selection. We found that among-population variation in dewlap characteristics was best explained by genetic ancestry. This result was supportd by genome-wide association mapping, which identified several ancestry-specific loci associated with dewlap traits. Despite the

strong imprint of this aspect of the invasion history on dewlap variation, we also detected significant relationships between dewlap traits and local environmental conditions. However, we found limited evidence that dewlap-associated genetic variants have been subject to selection. Our study emphasizes the importance of genetic ancestry and admixture in shaping phenotypes during biological invasion, while leaving the role of selection unresolved, likely due to the polygenic genetic architecture of dewlaps and selection acting on many genes of small effect.

Keywords:

Anolis; genetic ancestry; invasive species; natural selection; invasion history; dewlap

Introduction

Biological invasions enable researchers to conduct studies at large spatial and temporal scales that capture substantial environmental variation, facilitating the ability to observe ecological and evolutionary processes over contemporary timescales (Sakai et al., 2001; Sax et al., 2007; Lawson et al., 2011; Hodgins et al., 2018). When non-native populations encounter new environments in terms of predators, competitors, or abiotic conditions, this variation can relax selection experienced in their native range and/or impose novel selective pressures (Sakai et al., 2001; Lee, 2002; Bock et al., 2015, 2021). Invasions have provided many recent examples of rapid adaptation (e.g., Colautti & Barrett, 2013; Stern & Lee, 2020; Battlay et al., 2023). Previous studies have demonstrated phenotypic shifts in non-native species driven by natural selection occurring over the course of tens to hundreds of generations (e.g., Huey et al., 2000; Shine, 2011; Colautti & Barrett, 2013; Bock et al., 2018). Yet not all invasions result in rapid adaptation, even when non-native populations experience novel environments, due to a variety of factors such as a lack of associated selective pressures, little relevant genetic variation, or possible genetic constraints (e.g., Alexander & Edwards, 2010; Bock et al., 2021, Baeckens et al., 2023, Bock et al., 2023).

In addition to examples of rapid adaptation, studies of biological invasions have revealed the importance of the invasion history for patterns of demographic, genetic and phenotypic variation (e.g., Kolbe et al., 2004; Cristescu, 2015). Invasion history includes the contribution to genetic ancestry through the location and number of source populations in the native range (Kolbe et al., 2004, 2007a), the spread of populations in the non-native range (e.g., leading to ‘expansion load’; Peischl et al., 2013), and the extent of admixture (i.e., intraspecific hybridization of previously isolated sources) within non-native populations (Rius & Darling, 2014; Bock et al., 2021), among other factors. As a result, genetic and phenotypic variation can increase or decrease in invasive populations during an invasion. For example, admixture will often increase variation (Kolbe et al., 2004, 2008; Rius & Darling, 2014), whereas random genetic drift will decrease variation through founder effects and population bottlenecks (Dlugosch & Parker, 2008; Ficetola et al., 2008; Zhu et al., 2017). The invasion history is expected to have a strong effect on patterns of genetic and phenotypic variation within and among non-native populations, and can strongly bias the interpretation of drivers of evolution during invasions, when not properly accounted for (Keller & Taylor, 2008; Colautti et al., 2009; Hodgins et al., 2018). Therefore, understanding

evolution in introduced populations will often require elucidating the combined effects of invasion history and adaptation to environmental conditions encountered in the novel range.

The biological invasion of the brown anole lizard (*Anolis sagrei*) provides an excellent opportunity to test hypotheses for phenotypic evolution among non-native populations. Native to the northern Caribbean—Cuba, Bahamas, Cayman Brac and Little Cayman—the brown anole is a very successful invasive lizard that has been repeatedly introduced to Florida (USA) starting in the late 19th century (Garman, 1887) and expanding rapidly beginning in 1950s (Campbell, 1996). At least eight introduction events from genetically distinct native-range populations have resulted in non-native populations with greater genetic diversity than those observed in the native range (Kolbe et al., 2004, 2007a, 2008; Bock et al., 2021). Also, non-native Florida populations are more morphologically variable/span> in body size and shape, number of toepad lamellae, and number of scales compared to native Cuban populations (Lee, 1992; Kolbe et al., 2007a). This increased phenotypic and genetic variation may be acted upon by natural selection, which could promote evolution and facilitate invasion success (e.g., Shine 2011, but see Jaspers et al., 2021). Introduced populations differ significantly from each other in genetic variation and certain morphological traits (Kolbe et al., 2007a, 2008; Bock et al., 2021). Thus, the invasion history may dominate patterns of phenotypic and genetic variation in these non-native populations. Indeed, genetic ancestry rather than local adaptation better explains variation among non-native brown anole populations in morphology and water loss traits (Kolbe et al., 2007a; Bock et al., 2021; Baeckens et al., 2023). Moreover, novel genetic interactions that result from hybridization (e.g., Bock et al., 2021) and high linkage disequilibrium in chromosomal segments of reduced recombination (i.e., Bock et al., 2023) may play a role in constraining adaptive responses in the invasive range.

Given the lack of previous evidence for local adaptation among non-native brown anole populations, we wanted to focus on a phenotypically and genetically complex trait that is subject of multiple selective pressures to increase the chance of detecting evidence of natural selection. We therefore examined evolutionary change across the invasive range in the iconic *Anolis* signaling ornament: the dewlap. Dewlaps are extendable structures located on the throat of anoles that differ in size, shape, color, and patterning at both the inter- and intraspecific levels (Losos, 2009). This multifaceted signaling structure often plays an important role in territory establishment and defense (e.g., Fleishman, 1992), reproductive interactions (e.g., Crews, 1975), species recognition (e.g., Rand & Williams, 1970; Losos, 1985), and predator deterrence (e.g., Leal & Rodríguez-Robles, 1995; Leal & Rodríguez-Robles, 1997a,b). Considerable evidence supports that the dewlap is subject to a variety of selection pressures (Leal & Fleishman, 2002, 2004; Vanhooydonck et al., 2009; Ng et al., 2013a; Driessens et al., 2017). Previous research has shown strong, albeit contrasting, relationships between environmental conditions and dewlap design in native populations of *Anolis* lizards (Leal and Fleishman, 2002, 2004; Ng et al., 2013a; see Discussion for details). For brown anoles, native-range populations inhabiting mesic environments had primarily marginal dewlaps (i.e., red or orange covering most of the dewlap with yellow along the outer margin), showing high reflectance in red, whereas lizards occupying xeric environments had a higher

proportion of solid dewlaps with higher ultraviolet (UV) reflectance (Driessens et al., 2017). These results show that *Anolis* dewlap phenotypes are associated with variation in environmental conditions, likely resulting from differential selection on signal effectiveness in response to climatic conditions and physical habitat characteristics (Endler, 1992, 1993) as well as interactions with competitors, predators, and conspecifics (Cole, 2013).

In this study, we investigated multiple aspects of a complex trait in brown anole populations across a large portion of its non-native range in the southeastern United States. Our goal was to determine whether among-population variation in aspects of dewlap design can be best explained by environmental conditions (consistent with local adaptation), genetic ancestry, or a combination of both factors. Specifically, we tested whether variation in dewlap characteristics (i.e., color, pattern and size) were associated with 1) differences in prevailing environmental conditions (i.e., temperature, precipitation, and light conditions) and 2) genetic ancestry as measured by the relative contribution of genome-wide SNP variation inherited from different native-range source populations (Kolbe et al., 2004, 2007a, 2008, Bock et al., 2021). We complemented the latter ancestry-based tests with genome-wide trait association analyses, taking advantage of recent analytical developments that allow ancestry-specific associations to be detected along the genome (e.g., Skotte et al., 2019). Further, we relied on F_{ST} outlier analyses and genotype-environment association analyses, which can identify loci involved in adaptation. The phenotypically diverse and putatively polygenic nature of complex traits, such as the *Anolis* dewlap, afford an excellent opportunity to assess whether changing environmental conditions during an invasion shape phenotypic variation in ways consistent with natural selection. The brown anole invasion is a particularly useful case because previous studies of morphological and physiological traits have failed to provide evidence of adaptation during the invasion (i.e., Kolbe et al., 2007a, Bock et al., 2021, Baeckens et al., 2023, Bock et al., 2023). A better understanding of the evolutionary dynamics during biological invasions is useful for predicting future impacts of invasive species, especially as global environments continue to change rapidly.

Materials and Methods

Study sites and sampling

We sampled 13-28 brown anoles from each of 30 populations in southeastern United States from Florida (N = 28 sites) and Georgia (N = 2 sites; Table S1). Sites were organized along three latitudinal transects (Figure S1), completed during three field trips in March-July 2018. Sampling was limited to natural habitats with variable understory light conditions and no evidence of artificial structures. However, we sampled two populations (i.e., LOW and TIF; Table S1) from landscaped vegetation around hotel grounds due to low lizard densities in these areas. In all, we obtained 589 adult males, which were transported to the animal care facility of Harvard University. We kept the lizards for 5-9 weeks in the lab under uniform conditions in individual enclosures (see De Meyer et al., 2019 for a detailed enclosure description), during which time they were measured for a range of related projects. Dewlap characteristics were scored for a subset of 570 lizards at 10-30 days after arrival from

the field. All procedures described here for housing and measuring lizards were approved by the Harvard University Institutional Animal Care and Use Committee (IACUC protocol # 26-11).

Spectral data acquisition

Dewlap reflectance was measured with an Ocean Optics USB4000 spectrometer, a pulsed Xenon light source (PX-2, Ocean Optics), and a reflectance probe encased in a black anodized aluminum sheath. The reflectance probe was set at 45º to prevent specular reflection (i.e., glare; Endler, 1990). For each lizard, we collected reflectance data at three points: one in the center of the dewlap and two along the edge (Figure S2a). Dewlaps were extended using stainless-steel, reverse-action forceps. For each of the three points on the dewlap, we took three repeated measurements, resulting in nine measurements per individual. We calibrated the spectrometer after every three measurements using a Spectralon white and black standard and measured reflectance from 300 (ultraviolet, UV) to 700 nm (red) in 10-nm intervals (Cuthill et al., 1999). We included the UV spectral range since *Anolis* lizards have the capacity to perceive UV signals (Fleishman et al., 1993; Fleishman & Persons, 2001).

Spectral data processing

Spectrophotometric data were processed to reduce noise, remove technical artifacts, and analyze reflectance spectra using the package *pavo* (Maia et al., 2013) in R v.3.6.1 (R Development Core Team, 2011). Raw spectra were smoothed using the *procspec* function, which applies the LOESS (Locally Weighted Scatterplot Smoothing) method with a quadratic regression and a Gaussian distribution. To normalize spectra and correct for negative values, we set the minimum value to zero and scaled up other values accordingly using the *procspec* function. We tested for repeatability of measurements taken at the same position on the dewlap using the R package *rptR* (Stoffel et al., 2017). Because all repeatability estimates were above 80%, we averaged repeated measurements using the *aggspec* function in *pavo*. We extracted four colorimetric variables: total brightness, cut-on wavelength (i.e., hue), UV reflectance, and chroma. Total brightness was calculated as the area under the “uncorrected” spectral curve from 300 to 700 nm. To determine the UV reflectance and cut-on wavelength (i.e., the midpoint between baseline and maximum reflectance; Cummings, 2007), we corrected the spectra for brightness by making the area under each curve equal to 1.0 (Endler, 1990). This correction allows for the identification of differences in spectral shape that are unrelated to brightness (Ng et al., 2013a).

Dewlap color composition and pattern

Each extended dewlap was photographed using a Nikon D3300 (24.2 MP) digital camera on a white background under standardized room lighting conditions in the lab. We included a color standard (i.e., X-rite Mini ColorChecker® Classic) and a ruler for scale. Images were calibrated using the *colorChecker* function in the R package *patternize* (Van Belleghem et al., 2018). This function calculates a second order polynomial regression between the observed and expected RGB (red, green, and blue) values and performs the calibration of the image.

Because some dewlaps are a mixture of colors and the spectral data only represent three points on the dewlap, we also wanted to quantify the proportion of each color present in each dewlap. We determined the RGB values of the colors present in each pixel (size □ 0.007 mm) of the dewlap image using Color Inspector 3D (Barthel, 2006), a plugin for ImageJ (Rasband, 2012). This plugin displays the distribution of colors of an image within a 3D color space. We extracted the RGB values and their frequency and imported them to R. We obtained a list of known colors with their respective RGB values using the base R functions *colors* and *col2rgb*. Then, we classified dewlap RGB values for each pixel to color categories using Euclidean distance, which determines the nearest known color in RGB-space. Thisuantitative measure of color composition was calculated as the percent of red, orange, and yellow present in each dewlap.

Brown anole dewlaps vary from a single color to some combination of red, orange, and yellow-colored patches. A previous study of dewlap variation in the native range of the brown anole categorized dewlap patterns into two types (Driessens et al., 2017). ‘Solid’ dewlaps are uniformly colored and may contain a distinct marginal color, such as a reddish color covering most of the dewlap with a yellowish color along the outer margin (Figure S2b). ‘Spotted’ dewlaps have yellowish spots scattered across the reddish center and may also contain a yellow outer margin (Figure S2c). We scored dewlaps from non-native populations in our study using these same two categories to facilitate comparison to the native range analysis in Driessens et al. (2017).

Dewlap size

We measured dewlap area and perimeter from digital photos in ImageJ. Dewlap area and perimeter were measured by creating line segments throughout the border of the dewlap, ultimately forming a polygon and obtaining the area and perimeter of it. We measured the dewlap for each lizard twice to verify the repeatability of this method, which was 1.0. We used a digital x-ray system to capture skeletal images from euthanized lizards. Using ObjectJ, a plug-in for ImageJ, we estimated of body size by measuring snout-vent length (SVL), the distance from the tip of the snout (i.e., the edge of the soft tissue) to the final vertebrae that had forward-facing arms. SVL values were then log-transformed and regressed against log-transformed dewlap area and perimeter. The resulting residual values represent body size-adjusted dewlap size.

Environmental data

To estimate the amount of light filtered through the forest canopy, we took hemispherical photos with a 180º fisheye lens at the location where each lizard was first observed. Canopy photos were analyzed in Hemispherical_2.0, a macro for ImageJ, which calculates the percentage of pixels that are open sky (Beckschäfer, 2015).

We characterized environmental variation using Geographic Information System (GIS) climate layers interpolated from average monthly climate data from weather stations with a spatial resolution of about 1 km^2 (WorldClim database; Hijmans et al., 2005). For each sampled locality, we extracted two bioclimatic variables that have been considered important for explaining dewlap color variation in anoles: annual precipitation and annual mean temperature (Williams, 1974; Ng et al., 2013a; Driessens et al., 2017).

Statistical analyses

Reflectance spectra can be interpreted as a multivariate phenotype, where reflectance values at each discrete wavelength are a variable. Therefore, dewlap color can be represented in a multidimensional color space. To reduce the dimensionality of the spectral data, we binned reflectance values into 10-nm bins using the *procspec* function in *pavo* (Maia et al., 2013). Each of the three positions on the dewlap where we took spectral readings was included as a separate variable and repeated measurements at each position were averaged. We used the base R function *prcomp* to conduct a principal component analysis (PCA) on 123 variables representing the reflectance spectra.

We conducted linear mixed effect models using *lme4*, *lmer* and *lmerTest* packages in R (Bates et al., 2015; Kuznetsova et al., 2017). For these models, we assigned principal component (PC) axes 1 or 2, which includes all colorimetric variables across thepectral range, as the response variables. Further, percent Western Cuba ancestry (see ‘Population structure and genetic diversity’ section below) was included as a fixed factor along with the covariates annual mean temperature, annual mean precipitation, and canopy openness. We also included site as a random effect to account for variation among populations not related to our main hypotheses. To further investigate dewlap variation, we used models with the same covariates, as well as fixed and random effects as previously described to evaluate individual variables describing aspects of the dewlap: UV reflectance, total brightness, and hue across the three dewlap positions; color composition of red, orange, and yellow; and dewlap size (i.e., area and perimeter). We log-transformed data to improve normality when appropriate.

We performed a generalized linear model, specifically a binomial logistic regression, to identify whether any variables predict dewlap pattern (i.e., solid or spotted) using the base R function *glm*. The predictor variables were Western Cuba ancestry, canopy openness, annual mean temperature, and annual mean precipitation. All statistical analyses were performed in R.

Genome-wide SNP genotyping

We used the same samples and quality-filtered reads included in our previous study on the genetic architecture of limb length in *A. sagrei* (Bock et al., 2021). This sampling includes the *A. sagrei* males used here for dewlap measurements, non-native population samples obtained earlier in the invasion (i.e., in 2003), and samples from the native range of *A. sagrei*. Using quality-filtered reads for all samples (see detailed methods in Bock et al.,

2021), we repeated the SNP calling and variant filtering steps based on version 2.1 of the *A. sagrei* genome, which recently became available (Geneva et al., 2021). Reads were aligned to the genome using the dDocent v2.2.20 pipeline (Puritz et al., 2014), and SNPs were called using Freebayes v. 1.3.2 (Garrison & Marth, 2012).

Filtering of the resultant variant calls was implemented using vcflib (https://github.com/vcflib/vcflib) and consisted of sequential steps based on number of alleles (i.e., keeping only biallelic markers), type of variant (i.e., keeping only SNPs), read mapping quality (i.e., using SNPs with a MAPQ score > 20), and depth of sequencing (i.e., keeping only genotypes with DP > 7). For the remaining filtered SNPs, we used BCFtools v.1.9 (Narasimhan et al., 2016) to subset genotypes corresponding to the sequenced *A. sagrei* individuals obtained in 2018 from Florida and Georgia, for which dewlap trait data was also available (*N* = 561). Of the 561 samples, nine were sequenced in duplicate, resulting in 570 total sequencing libraries. We then kept only SNPs with data at more than 70% of samples and only SNPs with a minor allele frequency > 1%, and calculated identity-by-state (IBS) between samples using the SNPrelate R package (v. 1.19.4; Zheng et al., 2012). Following previous studies (e.g., Bock et al., 2021), we relied on IBS values between DNA replicates to estimate the rate of genotyping errors in our dataset. We then kept one replicate per sample and repeated the 70% call rate and minor allele frequency filters described above across all 561 genetically distinct samples. Finally, we removed one sample that had missing data at more than 30% of the final filtered SNPs, keeping the remaining 560 genotypes for downstream analyses.

Of the resulting filtered SNPs, we removed candidate gametolog SNPs following Bock et al. (2021). These gametolog SNPs occur on the X chromosome of *A. sagrei* (Geneva et al., 2021) and are a result of homology between the X chromosome (i.e., scaffold 7 in the *A. sagrei* v2.1 genome assembly) and the Y chromosome, which is currently not included in the genome assembly. After gametolog removal, we excluded markers that were in strong linkage disequilibrium (i.e. $r^2 > 0.4$), by scanning the genome in 5,000 SNP windows, using '--indep-pairwise' option in PLINK (v1.9; Purcell et al., 2007). We then kept all SNPs located on the largest 14 scaffolds of the genome assembly, which correspond to the known number of chromosomes for *A. sagrei* and cover more than 99% of the total assembly length (Geneva et al., 2021).

Population structure and genetic diversity

To summarize population structure, we relied on all LD-filtered autosomal SNPs and used Bayesian clustering as implemented in STRUCTURE v.2.3.4 (Pritchard et al., 2000). We considered *K* values from 1 to 10. For each *K* value, we used 20 independent replicates. Each replicate used the first 150,000 iterations as burn-in, followed 150,000 MCMC repetitions. We then used the *pophelper* (v.2.3.0; Francis, 2017) R package to estimate the most likely number of clusters in our data based on the delta K method (Evanno et al., 2005) and to plot the STRUCTURE results. We supplemented these analyses with a discriminant analysis of principal components

(DAPC) performed using the *adegenet* R package (v. 2.1.1; Jombart & Ahmed, 2011). We further calculated heterozygosity as the percent heterozygous SNPs out of all SNPs with data for a given individual.

Genome-wide association mapping for dewlap traits

The genome-wide association study (GWAS) was based on all LD-filtered markers. Prior to GWAS, missing data was imputed using BEAGLE v5.0 (Browning & Browning, 2016) at default settings. To investigate correlations among the 11 traits that capture dewlap size (i.e., area and perimeter) and color (i.e., hue, total brightness, mean brightness, UV chroma, red chroma, yellow chroma, and composition of red, orange, or yellow), we first used the *ggcorrplot* R package (v. 0.1.3; Kassambara, 2019). The GWAS was then performed using two complementary approaches, which we refer to as the "standard GWAS" and the "ancestry-specific GWAS". The standard GWAS consisted of a linear mixed model implemented in GEMMA (Zhou & Stephens, 2012). We first used GEMMA to calculate 10 relatedness matrices, by excluding SNPs from one chromosome at a time (i.e., each matrix was based on SNPs from 9 chromosomes). The GWAS for markers on a given chromosome was then performed using the relatedness matrix that excluded markers on that same chromosome. This approach should improve power to detect associations, given that the relatedness matrix does not include markers that are in linkage disequilibrium with the marker being tested (Cheng et al., 2013). We then obtained *P* values from the Wald test as outputted by GEMMA.

The ancestry-specific GWAS was conducted in asaMap (Skotte et al., 2019). To control for the confounding effect of population structure, we relied on the first 10 PCs from a PCA computed using the *adegenet* R package (v. 2.1.1; Jombart & Ahmed, 2011), which were included as covariates in the asaMap analysis. The PCA was based on all LD-filtered autosomal SNPs. The asaMap software performs eight association tests, with and without different ancestry-specific effects considered for two ancestral populations (Skotte et al., 2019). Following asaMap manual recommendations, we estimated genome-wide ancestry proportions of each sample, as well as SNP allele frequencies for each ancestral population using ADMIXTURE v. 1.3.0 (Alexander et al., 2009). For each dewlap trait, we obtained genome-wide *P* values for all tests and selected the test with the strongest association (i.e., the lowest observed *P* value among all tested SNPs), following Bock et al., (2021).

For both the standard and the ancestry-specific GWAS results, we used the *GenABEL* R package (Aulchenko et al., 2007) to calculate the lambda genomic inflation factor (λ), and account for any remaining *P* value inflation, which can be caused by unaccounted population stratification. Genome-wide significance thresholds were then set using the Bonferroni method (0.05/total SNPs used for the association test), which is the most conservative option used in association studies (e.g., Duggal et al., 2008; Kaler & Purcell, 2019). We also considered a suggestive genome-wide significance threshold (1/total SNPs used for the association test; Duggal et al., 2008), for which one false positive per GWAS is expected. To visualize GWAS results, we used Manhattan plots, made in R v.4.1.0 using publicly available scripts (https://danielroelfs.com/blog/how-i-create-manhattan-plots-using-ggplot/). Finally, to estimate the effect size of associations, we build linear models in R. These models had

number of alternative alleles (i.e., alleles different from those incorporated in the reference genome) at the lead GWA SNP as the predictor variable, and the corresponding dewlap trait as the response variable. Effect sizes were then estimated as R^2 values, using the “summary” function in R.

To better understand the observed effect of ancestry on dewlap traits, we next focused on results of the ancestry-specific GWAS. Specifically, we investigated how dewlap traits vary among genotype classes for ancestry-specific associations that passed the Bonferroni or suggestive significance thresholds. For this, we stratified the invasive *A. sagrei* samples based on ancestry, using a cutoff of 70% Western Cuba ancestry, as inferred using the STRUCTURE analysis. Because of the genetic makeup of invasive *A. sagrei* populations across thsoutheastern United States, this approach partitions samples into two groups, one with limited hybridization (i.e., Western Cuba ancestry samples) and another with frequent hybrids for which Central-eastern Cuba ancestry predominates (see also Bock et al., 2021).

Identifying the signature of local adaptation for dewlap-associated SNPs

To determine whether SNPs associated with dewlap traits are also involved in local adaptation of invasive *A. sagrei* populations, we combined F_{ST} outlier analyses and genotype-environment association analyses. The F_{ST} outlier approach aimed to determine whether dewlap-associated SNPs make a large contribution to population genetic differentiation in invasive *A. sagrei.* We followed the approach described in Bock et al. (2021) for the same set of populations as those used for dewlap measurements here. Briefly, we used VCFtools (v. 0.1.16; Danecek et al., 2011) to calculate SNP-based F_{ST} among 15 independent population pairs found in our dataset. For this, we relied on the full LD-filtered SNP set. We then compared F_{ST} values for all dewlap-associated SNPs with F_{ST} values observed for an equal number of randomly selected non-dewlap SNPs. For this, we used a linear model in R, which had population pair and locus category (i.e., dewlap or non-dewlap SNP) as predictor variables, and F_{ST} values as the response variable. As well, we designated as F_{ST} outliers those values that were in the top 5% of the empirical distribution, for each of the 15 population pairs. We then asked whether SNPs that are strongly associated with dewlap traits (i.e., those with the lowest inferred GWAS *P* value) are also repeatedly classified as F_{ST} outliers in multiple independent population pairs.

The genotype-environment association (GEA) analyses aimed to determine whether dewlap-associated SNPs are also associated with environmental variables that are important from the perspective of dewlap signal effectiveness. We followed the approach described in DeVos et al. (2023) and used a latent factor mixed model (LFMM), as implemented in the *lfmm* R package (v. 1.1; Frichot et al., 2013). To correct for the confounding effect of population structure, we set $K = 2$, which corresponds to the main genetic subdivision in our dataset (see ‘Population structure’ results below). Similar to the GWAS analyses described above, we adjusted the GEA *P* values based on the genomic inflation factor. We then relied on the *qvalue* R package (v. 2.30.0; Storey et al., 2015) to convert *P* values to *q* values and to identify genome-wide significant SNPs based on a false discovery

rate (FDR) of 5%. We used canopy openness as the environmental variable, given evidence of correlation between this metric and several of the dewlap traits (see 'Associations between the dewlap, genetic ancestry, and the environment' results below), and because this metric was considerably more variable than temperature or precipitation across our study populations (Figure S3). Finally, we compared the canopy openness GEA results with the standard GWAS results for dewlap total brightness. We focused on this trait for two reasons. First, dewlap brightness was correlated with canopy openness, as might be expected under local adaptation. Second, the GWAS for this trait revealed several ancestry-independent loci. Thus, we could exclude the confounding effects of genomic background, which may occur for loci identified using the ancestry-specific GWAS.

Results

Dewlap characteristics

Dewlap reflectance spectra revealed consistent patterns across populations (Figure S4). Despite individual variation in spectral characteristics, most lizards showed peak reflectance values between 600 to 700 nm wavelengths (Figure 1a). The relative intensity of UV wavelengths (300 to 400 nm) varied across individuals; dewlaps with greater proportions of yellow had higher UV reflectance values.

When comparing PC axes, dewlap reflectance showed strong differentiation between red and yellow-dewlapped lizards (Figure 1b). PC1 explained 63.7% of the variation, whereas PC2 explained 15.6%. High values of PC1 corresponded to relatively bright dewlaps, whereas low PC1 values corresponded to dull dewlaps. As for PC2, high values corresponded to red dewlaps and low values to yellow ones.

Population structure

The final LD-filtered SNP set contained 25,532 markers, of which 24,574 were located on the autosomes, and 958 were located on the X chromosome. Pairwise IBS values between samples averaged 91.52% (range 88.41%-97.01%). By contrast, IBS values estimated for DNA replicates approached 100% (average 99.91%; range 99.84%-99.96%), as expected if the genotyping error rate is low (i.e., below 0.16%, as estimated using the nine replicates). The STRUCTURE analyses performed using the 24,574 autosomal SNPs confirmed our previous results on genomic variation in these populations (Bock et al., 2021). The delta K criterion indicated that two genetic clusters (K = 2) are the best fit for our data (Figure S5a-c). As expected, all individuals were assigned ancestry from both genetically distinct clusters in varying proportions. Based on information from mtDNA sequences (Kolbe et al., 2004, 2007a) and genome-wide SNP data from the native range (Bock et al., 2021), these clusters can be interpreted as representative of ancestry from native lineages in Western and Central-eastern Cuba. Southern Florida populations have higher frequencies of Western Cuba ancestry, whereas central to northwestern Florida populations are highly admixed and contain higher frequencies of Central-eastern Cuba ancestry (Figure 2). Note, however, that DAPC indicated that a clustering of K = 3 could be a marginally better fit (Figures S6-S7).

Associations between the dewlap, genetic ancestry, and the environment

We found significant correlations between dewlap traits, genetic ancestry, and environmental variables. Dewlap variation as represented by PC1 and PC2 showed significant positive correlations with Western Cuba ancestry ($P < 0.001$, Table 1). As the frequency of Western Cuba ancestry increased, lizards exhibited brighter and redder dewlaps (Table 1, Figure 1b, Figure S8a,b). Additionally, PC1 was negatively correlated with canopy openness ($P = 0.001$; Table 1). As canopy openness increased (i.e., less canopy cover and lighter conditions), lizards exhibited darker dewlaps.

To further investigate the effects of genetic ancestry and environmental variation on distinct aspects of the dewlap and to follow-up on the PC-based analyses, we built separate models for each dewlap trait (i.e., univariate tests), including UV reflectance, total brightness, hue (cut-on wavelength), color composition (red, orange, yellow), area, and perimeter. Spectral colorimetric variables differed across dewlap positions; therefore, further analyses were also done by position (i.e., P1, P2 and P3). UV reflectance was negatively correlated with Western Cuba ancestry across dewlap positions (P1–edge, $P = 0.003$; P2–edge, $P = 0.017$; P3–center, $P = 0.003$; Table 1). Center UV reflectance showed significant positive correlations with canopy openness (P2, $P < 0.001$; P3, $P = 0.021$) and annual mean precipitation (P2, $P = 0.032$). Total brightness was positively correlated with Western Cuba ancestry (P1, P2 and P3, $P < 0.001$), negatively correlated with canopy openness (P1, $P < 0.001$; P2, $P = 0.028$), and negatively correlated with temperature (P3, $P = 0.028$). These univariate results were consistent with PC analyses, such that PC1 can be interpreted as brightness. Both PC1 (Figure S8a,l) and total brightness (Figure S8f-h,o,p) resulted in significant positive correlations with Western Cuba ancestry and negative correlations with canopy openness across dewlap positions (Table 1). PC2 and yellow composition were correlated with Western Cuba ancestry ($P < 0.01$; Figure S8); lizards with low PC2 values had yellow dewlaps (i.e., greater yellow composition) and low frequencies of Western Cuba ancestry. As for size, dewlap area and perimeter resulted in significant positive correlations with Western Cuba ancestry (Figure S8j-k) and negative correlations with canopy openness (Figure S8q,r; Table 1). The colorimetric variable hue (cut-on wavelength) was inconclusive due to a lack of model convergence.

Binomial logistic regression indicated that the probability of a lizard having a solid dewlap increased with Western Cuba ancestry ($P = 0.01$; Figure S9c). Although we observed variation in dewlap pattern across populations (Figs. S9-S10), this trait was not significantly correlated with any environmental variable (Table 2). Furthermore, we found no significant correlation between red color composition, genetic ancestry, and environmental variables. However, yellow color composition was negatively correlated with Western Cuba ancestry ($P = 0.004$, Figure S8i). These results are consistent with analyses of PC2. Lizards with low PC2 values had yellow dewlaps (Figure 1b) and low frequencies of Western Cuba ancestry (Figure 1b; Figure S8b).

Genetic architecture and selection tests for dewlap traits

Analysis of correlations among traits (Figure S11) revealed strong and significant correlations between our measurements of dewlap size (i.e., area and perimeter; r = 0.91) and between our measurements of dewlap brightness (i.e., mean and total dewlap brightness; r = 1). Moderate, albeit still significant, positive correlations were further revealed between dewlap hue, yellow chroma, and brightness, as well as between dewlap size and dewlap red chroma. Finally, dewlap UV chroma was negatively correlated with most dewlap traits (Figure S11).

The linear mixed model implemented in GEMMA (i.e., standard GWAS), identified seven loci distributed on chromosomes 2, 4, 6, 7, and 11 as significantly associated with the percent of red color (Figure 3, Table S2) at the Bonferroni-adjusted significance level. These associations were of moderate effect as estimated using percent variance explained (PVE; 3.5 to 9.6%; Figure 3). All other analyses using the GEMMA model did not reveal any associations with dewlap traits at the Bonferroni-adjusted significance level (Table S2). There were, however, SNPs that passed the suggestive genome-wide significance threshold. These suggestive associations were identified for nine of the dewlap traits, and were distributed on all macrochromosomes except chromosome 3, as well as on microchromosomes 9, 11, and 12 (Figure 3, Table S2).

The ancestry-specific GWAS identified one significant locus at the Bonferroni-adjusted level (Figure 4, Table S2), located on macrochromosome 2. This locus was associated with total and mean brightness with a moderate effect in samples of Western Cuba ancestry (PVE=3%; Figure 4), and a much smaller effect for samples in the Central-eastern Cuba ancestry group (PVE = 0.7%; Figure 4). Other ancestry-specific associations (N = 37 loci) were identified at the suggestive genome-wide threshold for 10 of the dewlap traits, distributed on chromosomes 1,2,4,5,6 and 11 (Figure 4; Table S2).

The F_{ST} values estimated for the 45 dewlap-associated SNPs (i.e., loci with both significant and suggestive associations with dewlap traits; Table S2) ranged from 0 to 0.62 (average 0.04), whereas F_{ST} for the 45 random SNPs ranged from 0 to 0.43 (average 0.03). The difference in F_{ST} between the dewlap-associated SNPs and the random SNPs was not, however, significant (P = 0.08; Figure S12a). As well, most dewlap-associated SNPs (i.e., 89%, or 40/45 SNPs) were not classified as F_{ST} outliers (Figure S12b). The remaining five dewlap-associated SNPs were F_{ST} outliers in one or two population pairs at most (Figure S12b). The GEA analysis identified one SNP on macrochromosome 2 at coordinate 22,431,024 that was significantly associated with canopy openness (q = 0.009; Figure S13a). However, this SNP was not associated with any dewlap traits (Figure S13b; Table S2), and it was not classified as an F_{ST} outlier, displaying F_{ST} values that ranged from 0 to 0.33 (average 0.05).

Discussion

Rapid adaptation is a common feature of biological invasions (e.g., Colautti & Barrett, 2013; Stern & Lee, 2020; Battlay et al., 2023). Counter to results for many invasions, previous studies of the brown anole in the

southeastern United States have revealed a lack of evidence for adaptation to the novel environmental conditions experienced there (Kolbe et al., 2007a, Bock et al., 2021, 2023, Baeckens et al., 2023). This is surprising given that the colonization of the non-native range in this species likely coincided with substantial changes in ecological interactions, as well as a shift from a tropical to a temperate climate. Consistent with previous studies of phenotypic evolution in the brown anole invasion, our results show that variation in dewlap characteristics among non-native populations is primarily explained by genetic ancestry. Admixture of multiple native-range lineages strongly influences the current genetic composition of non-native populations (Kolbe et al., 2004, 2007b, 2008, Bock et al., 2021). GWAS results corroborated these findings and indicated that most dewlap traits appear to have a complex genetic architecture. While we find that multiple aspects of the dewlap are related to local environmental conditions, genomic analyses did not indicate that dewlap-associated SNPs retain a signature consistent with local adaptation. Whether natural selection plays a role in signal divergence during the brown anole invasion thus requires further investigation. This study provides insight into the ongoing evolutionary processes occurring in biological invasions, highlighting the importance of genetic ancestry in brown anole dewlap variation among populations. Below, we put our findings in the context of previous studies of the brown anoles to better understand how populations have evolved during this invasion.

Genetic ancestry and its role in shaping dewlap phenotypes

Genetic clustering analyses revealed that genetic ancestry of invasive brown anoles can be summarized at a coarse level as a combination of two genetically distinct native lineages: Western Cuba and Central-eastern Cuba. Genetic ancestry had strong effects on several aspects of the dewlap; lizards with increasing Western Cuba ancestry have larger, brighter red dewlaps with lower UV reflectance and less yellow (Table 1, Figure 1b, S8a-k). As well, the probability of lizards having a solid dewlap increased with the frequency of Western Cuba ancestry (Figure S9c). This result is consistent with findings from the native range which, while based on more limited sampling, also find that Western Cuba populations of *A. sagrei* have a greater proportion of solid dewlaps, whereas Central-eastern Cuba populations have a greater proportion of spotted dewlaps (Driessens et al., 2017). These results point to an important role of genetic ancestry in shaping multiple dimensions of dewlap variation across invasive populations in this system.

Our genome-wide association analyses further explored the effect of genetic ancestry on dewlap variation. We identified several SNPs significantly associated with red coloration and brightness of dewlaps, and dozens of SNPs with suggestive associations with all dewlap traits (Figure 3, Table S2). Our finding that genetic ancestry has strong and widespread effects on dewlap differentiation among non-native populations is consistent with previous studies of invasive species (e.g., *Silene vulgaris*, Keller & Taylor, 2010; sticklebacks, Lucek et al., 2010). We previously used the same samples to identify a large-effect locus significantly associated with limb length in *A. sagrei* (Bock et al., 2021). Our results here indicate that the genetic architecture of the dewlap is likely different and more complex than that characterizing limb length, at least for *A. sagrei* of Cuban ancestry. This interpretation is further supported by among-trait correlations. While all limb length traits show strong and

significant pairwise correlations (Bock et al., 2021), dewlap traits are characterized by more moderate among-trait correlations that are occasionally non-significant (Figure S11).

The associations identified here between SNPs and dewlap traits should be interpreted with caution for two reasons. First, aside from associations reported for red composition and total and mean dewlap brightness, the strength of the association signal is reduced for any one SNP. Second, in-depth analyses of standard and ancestry-specific associations (Figures 3 and 4) revealed that genotype classes with the largest difference in trait values are also the ones witthe lowest sample size (e.g., genotype GG for Western Cuba ancestry, at Chr2: 166.587 Mb; Figure 4). Therefore, some of these results could be due to uneven sample sizes among genotype classes. With these caveats in mind, we note that the direction of the ancestry-specific effects reported here is consistent with our observations of the effect of Western Cuba ancestry on dewlap trait variation. Specifically, linear mixed effects models of dewlap traits based on genetic ancestry as well as the ancestry-specific GWAS indicated that Western Cuba ancestry is associated with increased brightness of dewlaps.

In many organisms, carotenoid pigments have been shown to be a source of variation in red, orange, and yellow ornamental coloration within and between species (reviewed in Toews et al., 2017). In most animal species, carotenoids cannot be synthesized and must be ingested. The extent to which dewlap color variation is influenced by nutritional condition has so far been investigated in a few anole species, *A. distichus* (Ng et al., 2013b) and *A. sagrei* (Steffen et al., 2010). Both studies found no difference in color between carotenoid and control treatments and dewlap coloration was heritable in *A. distichus* lizards. Moreover, biochemical investigations of dewlap pigment composition in several *Anolis* species have found that pterin pigments are important sources of coloration, although carotenoids were detected as well (Ortiz, 1962; Macedonia et al., 2000, Steffen & McGraw, 2007, 2009). In contrast to carotenoids, pterins are produced endogenously (reviewed in Andrade & Carneiro, 2021). Even so, identifying genes involved in pterin synthesis has been challenging because of the complexity of underlying biochemical pathways. For example, studies contrasting skin patches of different color in other reptiles have identified tens to hundreds of genes that are differentially expressed, and that are likely involved in the production of these pigments (e.g., McLean et al., 2017). Our finding that dewlap phenotypes are correlated with genome-wide estimates of genetic ancestry across non-native populations is in line with these previous studies and suggests a complex genetic architecture for dewlap traits.

Potential adaptation to light environments

We tested the hypothesis that dewlap phenotypes are correlated with environmental variation, which is expected under local adaptation. Supporting this prediction, we found significant relationships between multiple environmental variables and dewlap characteristics. Our strongest results show that dewlaps tend to be darker with relatively high UV reflectance as canopy openness (i.e., habitat light) increases. Also, we found that brown anoles occurring in habitats with greater precipitation had more UV reflectance. These findings are consistent with those obtained by previous studies in the native range of *A. sagrei*. Driessens et al. (2017) found that lizards

occupying open forest habitats had higher UV reflectance than populations inhabiting environments with little light exposure.

Studies in other *Anolis* species show different correlations between UV reflectance and the environment, suggesting the relationship between aspects of the dewlap and the local environmental conditions might be species specific. For example, Ng et al. (2013a) found no difference in UV reflectance among *A. distichus* populations inhabiting environments that differed in light characteristics. Also, Leal and Fleishman (2002, 2004) reported that *A. cristatellus* populations in Puerto Rico occupying closed forest habitats with little light penetration exhibit highly reflective and transmissive dewlaps with more UV reflectance. As light exposure increased (i.e., greater canopy openness), dark dewlaps with low UV reflectance were favored (Leal & Fleishman, 2004).

Several studies on local adaptation of *Anolis* dewlaps have contrasted populations in xeric and mesic habitats. These habitats differ in characteristics such as habitat light, temperature, or precipitation. We sampled brown anole populations across a latitudinal gradient throughout Florida and into southern Georgia. The southeast region of the United States is known to have relatively uniform climatic conditions within seasons. As expected, we found less variation in annual mean temperature and precipitation patterns among our sampled populations (Figure S3b,c) as compared to previous studies of tropical mesic and xeric habitats in Puerto Rico and the Dominican Republic (Leal & Fleishman, 2004, Ng et al., 2013a). Despite this reduced variation in temperature and precipitation, we found that lizards inhabiting cooler environments tend to have dewlaps with greater orange composition, which is consistent with previous studies of *A. distichus* (Ng et al., 2013a). While this may indicate convergent evolution of dewlap orange composition in relation to temperature in *A. distichus* and *A. sagrei*, the underlying mechanism is unknown.

In contrast to analyses at the trait level discussed above, analyses at the SNP level did not provide evidence of adaptation. Specifically, SNPs associated with dewlap traits had similar F_{ST} values as random genome-wide SNPs (Figure S12a). As well, dewlap-associated SNPs were rarely classified as F_{ST} outliers (Figure S12b). Moreover, the small number of dewlap-associated SNPs that do have extreme F_{ST} values are highly genetically differentiated in one or two population pairs at most (Figure S12b). These results therefore indicate that, if some of the dewlap-associated SNPs reported here are involved in local adaptation, their contribution is likely specific to a small number of populations, with different SNPs being recruited by natural selection in different populations. The genotype-environment association analyses further supported these results, indicating that dewlap-associated SNPs are not also associated with the environmental variables predicted to shape dewlap traits under local adaptation (Figure S13). Given evidence presented here that points to a complex genetic architecture for dewlaps and considering that invasive brown anole populations are highly genetically diverse, it is possible that adaptation occurs *via* small changes in allele frequency at a large number of loci. Identifying the genetic signature of natural selection at loci involved in the control of dewlap is needed to confirm the occurrence

of adaptation, as inferred from trait-environment corrlations. Achieving this task will be challenging, and will require much denser genome-wide data, in line with observations for other highly polygenic traits (Lowry et al., 2017).

In conclusion, the brown anole invasion allowed us to study the evolution of a complex signaling phenotype during a biological invasion, revealing how genetic ancestry strongly influences among-population variation in dewlaps in the non-native range. Our study supports the importance of invasion history and admixture in determining patterns of phenotypic divergence during biological invasions (Kolbe et al., 2004; Keller & Taylor, 2010). Although we found some evidence that aspects of the dewlap are correlated with environmental variation among non-native populations, which is consistent with previous studies and suggestive of local adaptation, the loci underlying these dewlap characteristics did not show a genetic signature consistent with the action of natural selection. Future studies should consider denser sampling of SNPs along the genome, which may allow the signature of natural selection to be recovered for these polygenic traits. Additionally, to better understand dewlap evolution in non-native brown anole populations, future studies should consider other potential sources of selection, including species recognition (Losos, 1985; Vanhooydonck et al., 2009; Baeckens et al., 2018a), sexual selection (Vanhooydonck et al., 2009), and intrasexual selection (i.e., male-male competition) (Vanhooydonck et al., 2005; Lailvaux & Irschick 2007; Baeckens et al., 2018b).

Acknowledgements

We thank Z. Chejanovski for help with fieldwork, as well as J. Breeze, C. Hahn, and M. Gage for help with lizard housing and care at Harvard University. Further, we thank the Genomics and Sequencing Center at the University of Rhode Island for help with constructing the sequencing libraries. This work was supported by the University of Rhode Island and National Science Foundation (NSF) grants (DEB-1354897) awarded to J.J.K., by NSF Graduate Research Fellowship under Grant No. 1747454 to J.N.P.A., by Belgian American Education Foundation (BAEF) to S.B., and by a Natural Sciences and Engineering Research Council of Canada Postdoctoral Fellowship, a Banting Postdoctoral Fellowship, and a Barbour award from the Harvard Museum of Comparative Zoology to D.G.B.

References

Alexander, J. M., Edwards, P. J. (2010). Limits to the niche and range margins of alien species. *Oikos*, 119(9), 1377-1386

Alexander, D. H., Novembre, J., & Lange, K. (2009). Fast model-based estimation of ancestry in unrelated individuals. *Genome Research*, *19*(9), 1655-1664.

Andrade, P., Carneiro, M. (2021). Pterin-based pigmentation in animals. *Biology Letters*, *17*(8), 20210221.

Aulchenko, Y. S., Ripke, S., Isaacs, A., & Van Duijn, C. M. (2007). GenABEL: an R library for genome-wide association analysis. *Bioinformatics*, *23*(10), 1294-1296.

Baeckens, S., Driessens, T., & Van Damme, R. (2018a). The brown anole dewlap revisited: Do predation pressure, sexual selection, and species recognition shape among-population signal diversity? *PeerJ*, 6, e4722.

Baeckens, S., Driessens, T., Huyghe, K., Vanhooydonck, B., Van Damme, R. (2018b). Intraspecific variation in the information content of an ornament: why relative dewlap size signals bite force in some, but not all island populations of *Anolis sagrei*. *Integrative and Comparative Biology*. *58*, 25-37.

Baeckens, S., Losos, J.B., Irschick, D.J., Kolbe, J.J., & Bock, D.G. (2023). Introduction history and hybridization determine the hydric balance of an invasive lizard facing a recent climate niche shift. *Evolution*, *77*(1), 123-137.

Barthel, K. U. (2006). 3D-data representation with ImageJ. *ImageJ Conference*.

Bates, D., Mächler, M., Bolker, B. M., & Walker, S. C. (2015). Fitting linear mixed-effects models using lme4. *Journal of Statistical Software*, *67*(1), 1-48.

Battlay, P., Wilson, J., Bieker, V.C. et al. (2023). Large haploblocks underlie rapid adaptation in the invasive weed *Ambrosia artemisiifolia*. *Nature Communications*. *14*, 1717.

Beckschäfer, P. (2015). Hemispherical_2.0. *Batch processing hemispherical and canopy photographs with ImageJ, User Manual.*

Bock, D. G., Baeckens, S., Pita-Aquino, J. N., Chejanovski, Z. A., Michaelides, S. N., Muralidhar, P., … & Kolbe, J. J. (2021). Changes in selection pressure can facilitate hybridization during biological invasion in a Cuban lizard. *Proceedings of the National Academy of Sciences*, *118*(42).

Bock, D.G., Baeckens, S., Kolbe, J.J., Losos, J.B. (2023). When adaptation is slowed down: Genomic analysis of evolutionary stasis in thermal tolerance during biological invasion in a novel climate. *Molecular Ecology*.

Bock, D. G., Caseys, C., Cousens, R. D., Hahn, M. A., Heredia, S. M., Hübner, S., … & Rieseberg, L. H. (2015). What we still don't know about invasion genetics. *Molecular Ecology*, *24*(9), 2277-2297.

Bock, D. G., Kantar, M. B., Caseys, C., Matthey-Doret, R., & Rieseberg, L. H. (2018). Evolution of invasiveness by genetic accommodation. *Nature Ecology & Evolution*, *2*(6), 991-999.

Browning, B. L., & Browning, S. R. (2016). Genotype imputation with millions of reference samples. *American Journal of Human Genetics*, *98*(1), 116-126.

Campbell, T. S. (1996). Northern range expansion of the brown anole Anolis sagrei in Florida and Georgia. *Herpetological Review*, *27*(3), 155-157.

Cheng, R., Parker, C. C., Abney, M., & Palmer, A. A. (2013). Practical considerations regarding the use of genotype and pedigree data to model relatedness in the context of genome-wide association studies. *G3: Genes, Genomes, Genetics*, *3*(10), 1861-1867.

Colautti, R. I., Barrett, S. C. H. (2013). Rapid adaptation to climate facilitates range expansion of an invasive plant. *Science*, *342*(6156), 364-366.

Colautti, R. I., Maron, J., & Barrett, S. C. H. (2009). Common garden comparisons of native and introduced plant populations: Latitudinal clines can obscure evolutionary inferences. Evolutionary Applications, *2*(2), 187-199.

Cole, G. L. (2013). Lost in translation: adaptation of mating signals in changing environments. *Springer Science Reviews*, *1*, 25-40.

Crews, D. (1975). Effects of different components of male courtship behaviour on environmentally induced ovarian recrudescence and mating preferences in the lizard, Anolis carolinensis. *Animal Behaviour*, *23*, 349-356.

Cristescu, M. E. (2015). Genetic reconstructions of invasion history. *Molecular Ecology*, 24, 2212-2225.

Cummings, M. E. (2007). Sensory trade-offs predict signal divergence in surfperch. *Evolution*, *61*(3), 530-545.

Cuthill, I. C., Bennett, A. T., Partridge, J. C., & Maier, E. J. (1999). Plumage reflectance and the objective assessment of avian sexual dichromatism. *The American Naturalist*, *153*(2), 183-200.

Danecek, P., Auton, A., Abecasis, G., Albers, C. A., Banks, E., Depristo, M. A., Handsaker, R. E., Lunter, G., Marth, G. T., Sherry, S. T., Mcvean, G., & Durbin, R. (2011). The variant call format and VCFtools. *Bioinformatics*, 27, 2156–2158.

De Meyer, J., Donihue, C. M., Scantlebury, D., Ng, J., Glor, R. E., Losos, J. B., & Geneva, A. J. (2019). Protocol for setting up and rearing a successful lizard room. *Anolis Newsletter VII*.

DeVos, T., Bock, D. G., & Kolbe, J. J. (2023). Rapid introgression of non-native alleles following hybridization between a native *Anolis* lizard species and a cryptic invader across an urban landscape. *Molecular Ecology*, 32(11), 2930–2944.

Dlugosch, K. M., & Parker, I. M. (2008). Founding events in species invasions: Genetic variation, adaptive evolution, and the role of multiple introductions. *Molecular Ecology*, 17(1), 431-449.

Driessens, T., Baeckens, S., Balzarolo, M., Vanhooydonck, B., & Huyghe, K. (2017). Climate-related environmental variation in a visual signalling device: the male and female dewlap in Anolis sagrei lizards. *Journal of Evolutionary Biology*, *30*(10), 1846-1861.

Duggal, P., Gillanders, E. M., Holmes, T. N., & Bailey-Wilson, J. E. (2008). Establishing an adjusted p-value threshold to control the family-wide type 1 error in genome wide association studies. *BMC Genomics*, *9*(1), 1-8.

Endler, J. A. (1993). Some general comments on the evolution and design of animal communication systems. *Philosophical Transactions of the Royal Society of London. Series B: Biological Sciences*, *340*(1292), 215-225.

Endler, J. A. (1990). On the measurement and classification of color in studies of animal color patterns. *Biological Journal of the Linnean Society*, *41*(4), 315-352.

Endler, J. A. (1992). Signals, signal conditions, and the direction of evolution. *The American Naturalist*, *139*, S125-S153.

Evanno, G., Regnaut, S., & Goudet, J. (2005). Detecting the number of clusters of individuals using the software STRUCTURE: A simulation study. *Molecular Ecology*, *14*(8), 2611-2620.

Ficetola, G. F., Bonin, A., & Miaud, C. (2008). Population genetics reveals origin and number of founders in a biological invasion. *Molecular Ecology*, *17*(3), 773-782.

Fleishman, L. J. (1992). The influence of the sensory system and the environment on motion patterns in the visual displays of anoline lizards and other vertebrates. *The American Naturalist*, *139*, S36-S61.
Fleishman, L. J., Loew, E. R., & Leal, M. (1993). Ultraviolet vision in lizards. *Nature*, *365*(6445), 397-397.
Fleishman, L. J., & Persons, M. (2001). The influence of stimulus and background colour on signal visibility in the lizard Anolis cristatellus. *The Journal of Experimental Biology*, *204*(9), 1559-1575.
Francis, R. M. (2017). pophelper: an R package and web app to analyse and visualize population structure. *Molecular Ecology Resources*, *17*(1), 27-32.
Frichot, E., Schoville, S.D., Bouchard, G., Francois, O. (2013). Testing for associations between loci and environmental gradients using latent factor mixed models. *Molecular Biology and Evolution*, 30, 1687–1699.
Garman, S. (1887). On West Indian Iguanidae and on West Indian Scincidae in the collection of the Museum of Comperative Zoology at Cambridge, Massachusets, USA. *Bulletin of the Essex Institute*, *19*, 25-50.
Garrison, E., & Marth, G. (2012). Haplotype-based variant detection from short-read sequencing. *arXiv* preprint arXiv:1207.3907.
Geneva, A. J., Park, S., Bock, D., Mello, P. de, Sarigol, F., Tollis, M., … & Losos, J. B. (2021). Chromosome-scale genome assembly of the brown anole (Anolis sagrei), a model species for evolution and ecology. *bioRxiv*. 2021.09.28.462146; doi: https://doi.org/10.1101/2021.09.28.462146.
Hijmans, R. J., Cameron, S. E., Parra, J. L., Jones, P. G., & Jarvis, A. (2005). Very high resolution interpolated climate surfaces for global land areas. *International Journal of Climatology: A Journal of the Royal Meteorological Society*, *25*(15), 1965-1978.
Hodgins, K. A., Bock, D. G., & Rieseberg, L. H. (2018). Trait evolution in invasive species. *Annual Plant Reviews Online*, 1, 459-496.
Huey, R. B. (2000). Rapid evolution of a geographic cline in size in an introduced fly. *Science*, 287(5451), 308-309.
Jaspers, C., Ehrlich, M., Pujolar, J. M., Kunzel, S., Bayer, T., Limborg, M.T., Lombard, F., Browne, W. E., Stefanova, K., & Reusch, B. H. (2021). Invasion genomics uncover contrasting scenarios of genetic diversity in a widespead marine invader. *Proceedings of the National Academy of Sciences, 118*(51).
Jombart, T., & Ahmed, I. (2011). adegenet 1.3-1: new tools for the analysis of genome-wide SNP data. *Bioinformatics*, *27*(21), 3070-3071.
Kassambara, A. (2019). ggcorrplot: Visualization of a correlation matrix using 'ggplot2'. *R package version 0.1, 3.*
Kaler, A.S., Purcell, L.C. (2019). Estimation of a significance threshold for genome-wide association studies. *BMC Genomics, 20*, 618.
Keller, S. R., & Taylor, D. R. (2008). History, chance and adaptation during biological invasion: Separating stochastic phenotypic evolution from response to selection. In *Ecology Letters*, *11*(8), 852-866.
Keller, S. R., & Taylor, D. R. (2010). Genomic admixture increases fitness during a biological invasion. *Journal of Evolutionary Biology*, *23*(8), 1720-1731.
Kolbe, J. J., Glor, R. E., Schettino, L. R., Lara, A. C., Larson, A., & Losos, J. B. (2004). Genetic variation increases during biological invasion by a Cuban lizard. *Nature*, *431*(7005), 177-181.
Kolbe, J. J., Larson, A., & Losos, J. B. (2007a). Differential admixture shapes morphological variation among invasive populations of the lizard Anolis sagrei. *Molecular Ecology*, *16*(8), 1579-1591.
Kolbe, J. J., Glor, R. E., Schettino, L. R., Lara, A. C., Larson, A., & Losos, J. B. (2007b). Multiple sources, admixture, and genetic variation in introduced *Anolis* lizard populations. *Conservation Biology*, 21(6), 1612-1625.
Kolbe, J. J., Larson, A., Losos, J. B., & de Queiroz, K. (2008). Admixture determines genetic diversity and population differentiation in the biological invasion of a lizard species. *Biology Letters*, *4*(4), 434-437.
Kuznetsova, A., Brockhoff, P. B., & Christensen, R. H. B. (2017). lmerTest Package: Tests in Linear Mixed Effects Models. *Journal of Statistical Software*, *82*, 1-26.
Lailvaux, S. P., & Irschick, D. J. (2007). The evolution of performance- based male fighting ability in Caribbean *Anolis* lizards. *American Naturalist*, 170(4), 573-586.
Lawson Handley, L. J., Estoup, A., Evans, D. M., Thomas, C. E., Lombaert, E., Facon, … & Roy, H. E. (2011). Ecological genetics of invasive alien species. *BioControl*, *56*(4), 409-428.
Leal, M., & Fleishman, L. J. (2002). Evidence for habitat partitioning based on adaptation to environmental light in a pair of sympatric lizard species. *Proceedings of the Royal Society. Series B: Biological Sciences*, *269*(1489), 351-359.
Leal, M., & Rodríguez-Robles, J. A. (1995). Antipredator responses of Anolis cristatellus (Sauria, Polychrotidae). *Copeia*, 155-161.
Leal, M., & Fleishman, L. J. (2004). Differences in visual signal design and detectability between allopatric populations of Anolis lizards. *The American Naturalist*, *163*(1), 26-39.
Leal, M., & Rodríguez-Robles, J. A. (1997a). Antipredator responses of the Puerto Rican giant anole, Anolis cuvieri (Squamata: Polychrotidae). *Biotropica*, *29*, 372-375.
Leal, M., & Rodríguez-Robles, J. A. (1997b). Signalling displays during predator-prey interactions in a Puerto Rican anole, Anolis cristatellus. *Animal Behaviour*, *54*(5), 1147-1154.
Lee, C. E. (2002). Evolutionary genetics of invasive species. *Trends in Ecology and Evolution*, *17*(8), 386-391.
Lee, J. C. (1992). Anolis sagrei in Florida: Phenetics of a Colonizing Species III. West Indian and Middle American Comparisons. *Copeia*, *4*, 942-954.
Losos, J. B. (1985). An experimental demonstration of the species-recognition role of *Anolis* dewlap color. *Copeia*, 905-910.

Losos, J. B. (2009). *Lizards in an Evolutionary Tree: Ecology and Adaptive Radiation of anoles*. University of California Press.

Lowry, D. B., Hoban, S., Kelley, J. L., Lotterhos, K. E., Reed, L. K., Antolin, M. F., & Storfer, A. (2017). Breaking RAD: An evaluation of the utility of restriction site-associated DNA sequencing for genome scans of adaptation. *Molecular Ecology Resources*, 17(2), 142–152.

Lucek, K., Roy, D., Bezault, E., Sivasundar, A., & Seehausen, O. (2010). Hybridization between distant lineages increases adaptive variation during a biological invasion: Stickleback in Switzerland. *Molecular Ecology*, 19, 3995-4011.

Macedonia, J. M., James, S., Wittle, L. W. & Clark, D. W. (2000). Skin pigments and coloration in the Jamaican radiation of *Anolis* lizards. *Journal of Herpetology*, 34, 99-109.

Maia, R., Eliason, C. M., Bitton, P. P., Doucet, S. M., & Shawkey, M. D. (2013). pavo: An R package for the analysis, visualization and organization of spectral data. *Methods in Ecology and Evolution*, *4*(10), 906-913.

McLean, C. A., Lutz, A., Rankin, K. J., Stuart-Fox, D., & Moussalli, A. (2017). Revealing the biochemical and genetic basis of color variation in a polymorphic lizard. *Molecular Biology and Evolution*, *34*(8), 1924-1935.

Narasimhan, V., Danecek, P., Scally, A., Xue, Y., Tyler-Smith, C., & Durbin, R. (2016). BCFtools/RoH: A hidden Markov model approach for detecting autozygosity from next-generation sequencing data. *Bioinformatics*, 32(11), 1749-1751.

Ng, J., Landeen, E. L., Logsdon, R. M., & Glor, R. E. (2013a). Correlation between anolis lizard dewlap phenotype and environmental variation indicates adaptive divergence of a signal important to sexual selection and species recognition. *Evolution*, *67*(2), 573-582.

Ng, J., Kelly, A. L., MacGuigan, D. J., & Glor, R. E. (2013b). The role of heritable and dietary factors in the sexual signal of a Hispaniolan *Anolis* lizard, *Anolis distichus*. *The Journal of Heredity*, 104(6), 862-873.

Ortiz, E., 1962. Drosopterins in the dewlap of some anoline lizards. *American Zoologist*, *2*(4), 545-546.

Peischl, S., Dupanloup, I., Kirkpatrick, M., & Excoffier, L. (2013). On the accumulation of deleterious mutations during range expansions. *Molecular Ecology*, *22*(24), 5972-5982.

Pritchard, J. K., Stephens, M., & Donnelly, P. (2000). Inference of population structure using multilocus genotype data. *Genetics*, *155*, 945-959.

Purcell, S., Neale, B., Todd-Brown, K., Thomas, L., Ferreira, M. A. R., Bender, D., … & Sham, P. C. (2007). PLINK: a tool set for whole-genome association and population-based linkage analyses. *American Journal of Human Genetics*, *81*(3), 559-575.

Puritz, J. B., Hollenbeck, C. M., & Gold, J. R. (2014). dDocent: A RADseq, variant-calling pipeline designed for population genomics of non-model organisms. *PeerJ*, 2, e431.

R Development Core Team, R. (2011). R: a language and environment for statistical computing. *R Foundation for Statistical Computing*.

Rand, A. S., & Williams, E. E. (1970). An estimation of redundancy and information content of anole dewlaps. *The American Naturalist*, *104*(935), 99-103.

Rasband, W. (2012). ImageJ. U. S. National Institutes of Health, Bethesda, Maryland, USA, *http://imagej.nih.gov/ij/*.

Rius, M., & Darling, J. A. (2014). How important is intraspecific genetic admixture to the success of colonising populations? In *Trends in Ecology and Evolution*, *29*(4), 233-242.

Sakai, A. K., Allendorf, F. W., Holt, J. S., Lodge, D. M., Molofsky, J., With, K. A., … & Weller, S. G. (2001). The population biology of invasive species. *Annual Review of Ecology and Systematics*, *32*(1), 305-332.

Sax, D. F., Stachowicz, J. J., Brown, J. H., Bruno, J .F., Dawson, M. N., Gaines, S. D., Grosberg, R. K., Hastings, A., Holt, R. D., Mayfield, M. M., O'Connor, M. I. & Rice, W. R. (2007). Ecological and evolutionary insights from species invasions. *Trends in Ecology and Evolution*, 22(9), 465-471.

Shine, R. (2011). Invasive species as drivers of evolutionary change: cane toads in tropical Australia. *Evolutionary Applications*, *5*(2), 107-116.

Skotte, L., Jørsboe, E., Korneliussen, T. S., Moltke, I., & Albrechtsen, A. (2019). Ancestry-specific association mapping in admixed populations. *Genetic Epidemiology*, *43*(5), 506-521.

Steffen, J. E., & McGraw, K. J. (2007). Contributions of pterin and carotenoid pigments to dewlap coloration in two anole species. *Comparative Biochemistry and Physiology, Part B*, 146: 42-46.

Steffen, J. E., & McGraw, K. J. (2009). How dewlap color reflects its carotenoid and pterin content in male and female brown anoles (*Norops sagrei*). *Comparative Biochemistry and Physiology – B Biochemistry and Molecular Biology*, 154, 334-340.

Steffen, J. E., Hill, G. E., & Guyer, C. (2010). Carotenoid access, nutritional stress, and dewlap color of male brown anoles. *Copeia*, *2010*(2), 239-246.

Stern, D. B., & Lee, C. E. (2020). Evolutionary origins of genomic adaptations in an invasive copepod. *Nature Ecology and Evolution*, 4, 1084–1094.

Stoffel, M. A., Nakagawa, S., & Schielzeth, H. (2017). rptR: repeatability estimation and variance decomposition by generalized linear mixed-effects models. *Methods Ecology and Evolution*, *8*(11), 1639-1644.

Storey, J. D., Bass, A. J., Dabney, A., & Robinson, D. (2015). Qvalue: Q-value estimation for false discovery rate control. R package version 2.0. http://github.com/jdsto rey/qvalue.

Toews, D. P. L., Hofmeister, N. R., & Taylor, S. A. (2017). The evolution and genetics of carotenoid processing in animals. *Trends in Genetics*, *33*(3), 171-182.

Van Belleghem, S. M., Papa, R., Ortiz-Zuazaga, H., Hendrickx, F., Jiggins, C. D., Owen McMillan, W., & Counterman, B. A. (2018). patternize: An R package for quantifying colour pattern variation. *Methods in*

Ecology and Evolution, *9*(2), 390-398.
Vanhooydonck, B., Herrel, A., Meyers, J. J., & Irschick, D. J. (2009). What determines dewlap diversity in Anolis lizards? An among-island comparison. *Journal of Evolutionary Biology*, *22*(2), 293-305.
Vanhooydonck, B., Herrel, A. Y., Van Damme, R., & Irschick, D. J. (2005). Does dewlap size predict male bite performance in Jamaican *Anolis* lizards? *Functional Ecology*, 19(1), 38-42.
Williams, E. E. (1974). Williams Report. *The Second Anolis Newsletter*, 1-10.
Zheng, X., Levine, D., Shen, J., Gogarten, S. M., Laurie, C., & Weir, B. S. (2012). A high-performance computing toolset for relatedness and principal component analysis of SNP data. *Bioinformatics*, *28*, 3326-3328.
Zhou, X., & Stephens, M. (2012). Genome-wide efficient mixed-model analysis for association studies. *Nature Genetics*, *44*(7), 821-824.
Zhu, B. R., Barrett, S. C. H., Zhang, D. Y., & Liao, W. J. (2017). Invasion genetics of Senecio vulgaris: loss of genetic diversity characterizes the invasion of a selfing annual, despite multiple introductions. *Biological Invasions 19*(1), 255-267.

Data Accessibility

Raw sequence data used for this project are available in the Sequence Read Archive (SRA) https://www.ncbi.nlm.nih.gov/sra (BioProject accession PRJNA737437). The scripts used for analyses, the dewlap trait data, the ancestry data, and the environmental data are available from FigShare (DOI: 10.6084/m9.figshare.24009063.v2).

Author contributions

J.N.P.A., D.G.B., and J.J.K. designed research; J.N.P.A., D.G.B., and S.B. performed research; J.N.P.A. and D.G.B. analyzed data; and J.N.P.A., D.G.B., S.B., J.B.L., and J.J.K. contributed to writing the paper.

Tables and Figures (with captions)

Tables

Table 1. Results of the linear mixed effects models performed to detect relationships between dewlap traits, Western Cuba ancestry, and environmental variables. Colorimetric variables (i.e., UV reflectance and total brightness) were obtained using edge (P1/P2) and center (P3) dewlap measurements. We log-transformed UV reflectance, total brightness, color composition (i.e., red, orange, yellow) and dewlap area to improve normality. Residual area represents body size-adjusted dewlap size. Hue (cut-on wavelength) was inconclusive due to lack of model convergence. Significant P-values are indicated with an asterisk (*).

Dewlap characteristic	Variable	Estimate	Std. Error	DF	T-statistic	P-value
P1–P3: Total reflectance (PC1)	Intercept	22.261	12.034	28.506	1.850	0.075
	Western Cuba ancestry	13.491	1.761	34.922	7.660	<0.001 *
	Canopy openness	-0.220	0.063	30.193	-3.498	0.001 *
	Temperature	-0.548	0.407	27.852	-1.346	0.189
	Precipitation	-0.008	0.007	26.827	-1.126	0.270
P1–P3: Total reflectance (PC2)	Intercept	-6.418	8.137	27.294	-0.789	0.437
	Western Cuba ancestry	5.654	1.130	44.282	5.005	<0.001 *
	Canopy openness	0.036	0.042	26.962	0.857	0.399
	Temperature	0.252	0.275	27.455	0.914	0.368
	Precipitation	-0.002	0.005	25.298	-0.394	0.697
P1 – UV reflectance	Intercept	-2.822	0.529	25.965	-5.333	<0.001 *
	Western Cuba ancestry	-0.236	0.074	41.966	-3.211	0.003 *
	Canopy openness	0.005	0.003	25.670	1.899	0.069
	Temperature	0.025	0.018	26.107	1.410	0.170
	Precipitation	0.001	<0.001	24.068	1.649	0.112
P2 – UV reflectance	Intercept	-2.164	0.385	25.384	-5.624	<0.001 *
	Western Cuba ancestry	-0.142	0.056	31.035	-2.521	0.017 *
	Canopy openness	0.008	0.002	26.931	3.883	<0.001 *
	Temperature	-0.006	0.013	24.787	-0.429	0.671
	Precipitation	0.001	<0.001	23.885	2.281	0.032 *
P3 – UV reflectance	Intercept	-2.367	0.372	25.188	-6.361	<0.001 *
	Western Cuba ancestry	-0.175	0.054	30.770	-3.217	0.003 *
	Canopy openness	0.005	0.002	26.734	2.449	0.021 *
	Temperature	0.023	0.013	24.593	1.824	0.080
	Precipitation	0.001	<0.001	23.702	1.108	0.279

P1 – Total brightness	Intercept	4.324	0.201	26.390	21.494	<0.001 *
	Western Cuba ancestry	0.060	0.029	36.690	2.071	0.045 *
	Canopy openness	-0.004	0.001	26.880	-4.022	<0.001 *
	Temperature	-0.005	0.007	26.170	-0.709	0.485
	Precipitation	<0.001	<0.001	24.640	0.005	0.996
P2 – Total brightness	Intercept	4.341	0.144	27.764	30.238	<0.001 *
	Western Cuba ancestry	0.138	0.021	33.595	6.570	<0.001 *
	Canopy openness	-0.002	0.001	29.559	-2.308	0.028 *
	Temperature	-0.006	0.005	27.079	-1.276	0.213
	Precipitation	<-0.001	<0.001	26.148	-1.969	0.060
P3 – Total brightness	Intercept	4.353	0.156	27.510	27.863	<0.001 *
	Western Cuba ancestry	0.113	0.023	32.530	4.908	<0.001 *
	Canopy openness	-0.002	0.001	29.590	-2.034	0.051
	Temperature	-0.012	0.005	26.750	-2.325	0.028 *
	Precipitation	<-0.001	<0.001	25.950	-0.548	0.588
Color composition: Red	Intercept	7.581	39.972	26.148	0.190	0.851
	Western Cuba ancestry	8.745	5.458	45.910	1.602	0.116
	Canopy openness	0.074	0.208	25.494	0.356	0.724
	Temperature	2.062	1.352	26.416	1.525	0.139
	Precipitation	-0.010	0.025	24.180	-0.386	0.703
Color composition: Orange	Intercept	4.715	0.708	26.005	6.660	<0.001 *
	Western Cuba ancestry	-0.118	0.099	39.781	-1.183	0.244
	Canopy openness	-0.005	0.004	25.885	-1.249	0.223
	Temperature	-0.048	0.024	25.984	-2.018	0.054
	Precipitation	<0.001	<0.001	24.189	0.415	0.682
Color composition: Yellow	Intercept	1.428	1.273	26.932	1.122	0.272
	Western Cuba ancestry	-0.527	0.172	49.084	-3.056	0.004 *
	Canopy openness	0.005	0.007	26.139	0.813	0.424
	Temperature	-0.010	0.043	27.279	-0.238	0.813
	Precipitation	<0.001	<0.001	24.874	0.970	0.341
Area	Intercept	0.448	0.159	26.790	2.809	0.009 *
	Western Cuba ancestry	0.088	0.022	43.020	3.978	<0.001 *
	Canopy openness	-0.002	0.001	26.460	-2.292	0.030 *
	Temperature	-0.011	0.005	26.790	-2.024	0.053
	Precipitation	<-0.001	<0.001	24.880	-1.547	0.135
Perimeter	Intercept	0.214	0.077	26.710	2.784	0.010 *
	Western Cuba ancestry	0.045	0.011	44.800	4.261	<0.001 *
	Canopy openness	-0.001	<0.001	26.210	-2.767	0.010 *
	Temperature	-0.004	0.003	26.820	-1.692	0.102
	Precipitation	-0.001	<0.001	24.760	-1.750	0.092

Table 2. Results of the binomial logistic regression model performed to detect relationships between dewlap pattern, Western Cuba ancestry, and environmental variables (i.e., temperature, precipitation, and canopy openness). We categorized dewlap patterns into two types; ‘solid’ dewlaps are uniformly colored and may contain a margin and ‘spotted’ dewlaps having yellowish spots scattered across the reddish center and may also contain a yellow outer margin. Significant P-values are indicated with an asterisk (*).

Variable	Estimate	Std. Error	Z-value	P-value
Intercept	2.489	2.295	1.085	0.278
Western Cuba ancestry	-0.910	0.337	-2.696	0.007 *
Canopy openness	-0.018	0.012	-1.413	0.158
Temperature	0.009	0.076	0.120	0.904
Precipitation	-0.002	0.001	-1.165	0.244

Figures

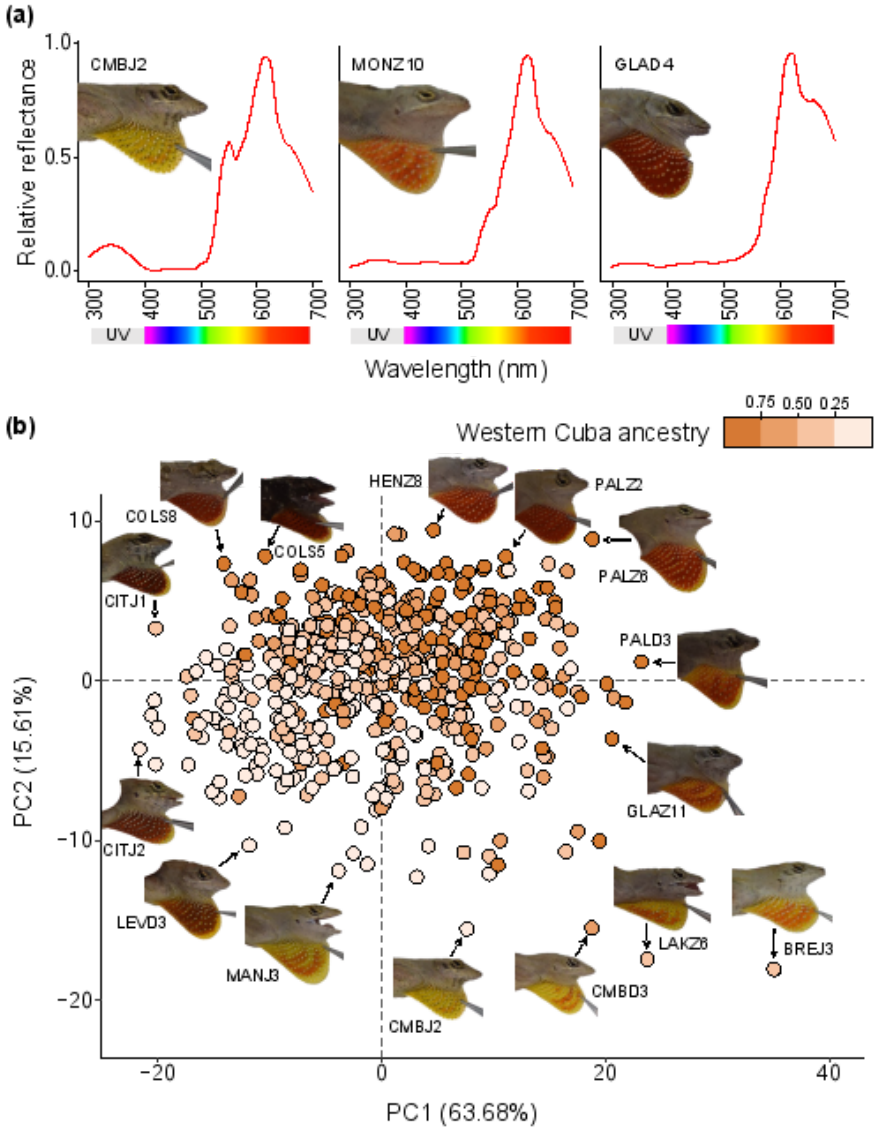

Figure 1. (a) Mean and standard deviation of three representative dewlap phenotypes. The area under the curve of each spectrum was normalized to one prior to averaging. Representative dewlap spectra per population can be found in Figure S4. (b) Results of a PCA for dewlap reflectance for all individuals. Spectral data for each dewlap position (P1, P2, P3) were included as separate variables divided into 10-nm intervals, resulting in 123 variables. Photos of lizards with their dewlaps extended represent the color variation along each PC axis. High values of PC1 correspond to relatively bright dewlaps, whereas low PC1 values correspond to dull dewlaps. As for PC2, high values correspond to red dewlaps and low values correspond to yellow ones. The shading of points corresponds to the proportion of Western Cuba ancestry inferred from the K = 2 STRUCTURE results (see Figure S5).

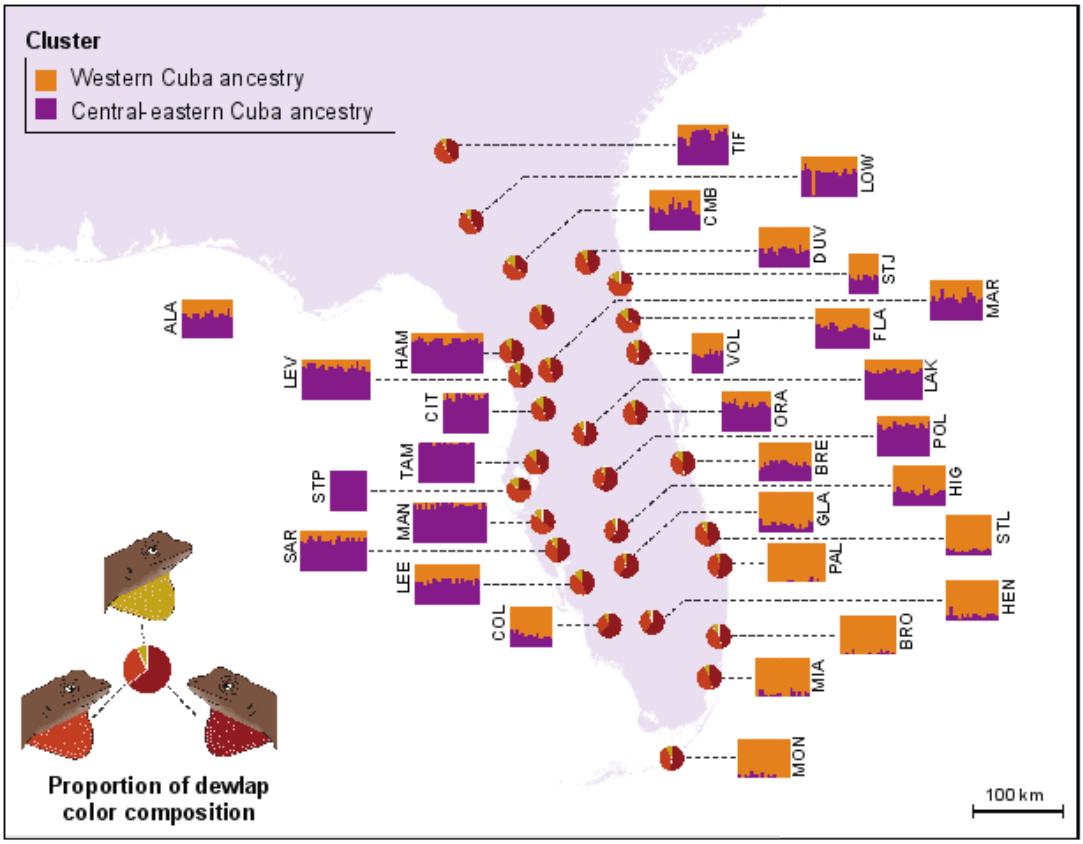

Figure 2. Geographical distribution of genetic ancestry for individuals from the STRUCTURE analysis. Each bar corresponds to one individual. The two genetic clusters are representative of Western Cuba (orange) and Central-eastern Cuba (purple) ancestry, based on information from previous studies using mitochondrial DNA sequences (Kolbe et al., 2004) and genome-wide SNP data (Bock et al., 2021). Pie charts represent the proportion of dewlap color composition across sampled populations.

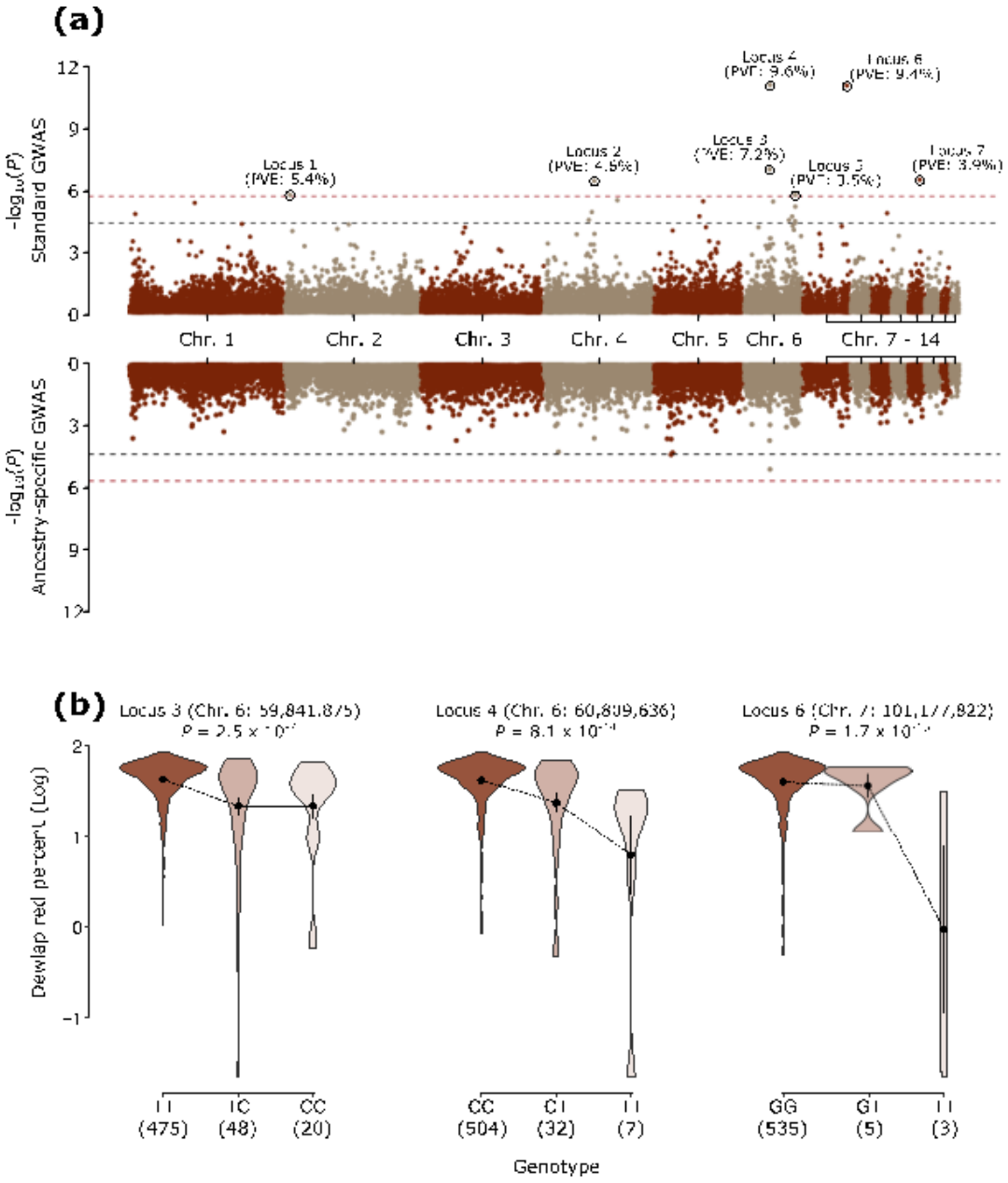

Figure 3. Genome-wide association results for percent red color in dewlaps. (a) Manhattan plots for the LMM implemented in GEMMA (top) and the ancestry-specific association model implemented in asaMap (bottom). The red dashed lines mark the genome-wide significance threshold calculated using the Bonferroni method. A more permissive suggestive significance level is shown using the black dashed lines. (b) Dewlap red percent (log-transformed) values shown for the three loci with the largest PVE. For each genotype class, points show the mean, and the black lines indicate standard error. The numbers shown in parentheses under each genotype class indicate sample sizes.

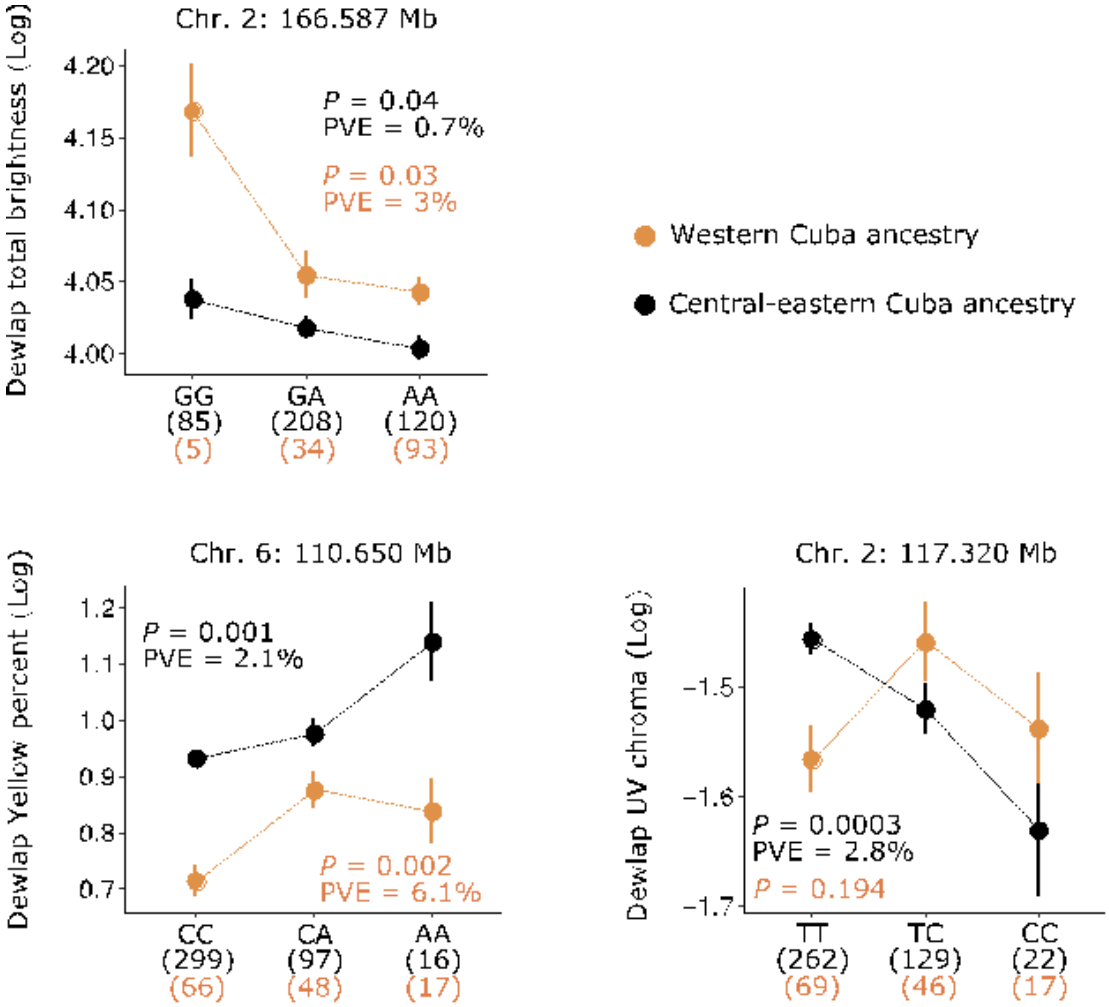

Figure 4. Ancestry-specific associations identified for dewlap traits. Only the three loci showing the strongest association signals are shown (all other associations are listed in Table S2). Of these, the association for dewlap brightness passed the Bonferroni significance threshold, whereas the other two loci passed the suggestive significance threshold. The effect of alleles at each SNP on trait values was calculated separately for the “Western Cuba ancestry” and the “Central-eastern Cuba ancestry” sample groups. Sample sizes for each sample group are given below each genotype.

1